BJPS

Brazilian Journal of
Pharmaceutical Sciences

http://dx.doi.org/10.1590/s2175-97902017000400191

Article

Synthesis, characterization and biological activity of a gold(I) triazenide complex against chronic myeloid leukemia cells and biofilm producing microorganisms

Melise Silveira Nunes[1], Litiérri Razia Garzon[1], Roberta Filipini Rampelotto[1], Maísa Kräulich Tizotti[1], Rosiéli Martini[1], Aline Locatelli[2], Marcelo Barbosa[3], Manfredo Hörner[1], Rosmari Hörner[1]*

[1]Federal University of Santa Maria (UFSM), Santa Maria, Rio Grande do Sul, Brazil, [2]University of Passo Fundo, Passo Fundo, Rio Grande do Sul, Brazil, [3]Universitary Hospital of Santa Maria (HUSM), Santa Maria, Rio Grande do Sul, Brazil

The enhancement of anti-leukemia therapy and the treatment of infections caused by multidrug-resistant pathogens are major challenges in healthcare. Although a large arsenal of drugs is available, many of these become ineffective, and as a result, the discovery of new active substances occurs. Notably, triazenes (TZCs) have been consolidated as a promising class of compounds, characterized by significant biological activity, especially antiproliferative and antimicrobial properties. The aim of this study is the synthesis and characterization of a new triazenide complex of gold (I), as well as the *in vitro* assessment of its antiproliferative activity against the K562 cell line (Chronic Myeloid Leukemia), and antibacterial activity against bacterial isolates of biofilm-producing coagulase-negative staphylococci. The combination of TZC with gold metal tends to have a synergistic effect against all biofilm-producing isolates, with Minimum Inhibitory Concentration values (MIC) between 32 and 64 μg mL^{-1}. It has also shown activity against K562 cell line, getting an IC_{50}=4.96 μM. Imatinib mesylate (Glivec) was used as reference, with IC_{50}=3.86 μM. To the best of our knowledge, this study represents the first report of the activity of a TZC complexed with gold ion in the oxidation state (I) against microorganisms that produce biofilm and K562 cells.

Keywords: Triazenes/synthesis/characterization/biological activity. TZC/Gold ion complexed. .Chronic myeloid leukemia. Antibacterial activity.

INTRODUCTION

Chronic myeloid leukemia (CML) is an hematologic malignancy characterized by excessive myeloid proliferation and the presence of a cytogenetic abnormality known as the Philadelphia chromosome (Ph), which occurs in 90% of CMLs, 20% of acute lymphocytic leukemia (ALLs) in adults, 5% of pediatric ALLs, and 1% of acute myeloid leukemia (AML) patients (Heim, Mitelman, 2009). This change stems from the reciprocal and balanced translocation between the long arms of chromosomes 9 and 22, t (9; 22) (q34; q11.2), resulting in BCR-ABL abnormal gene (Gora-Tybor, Robak, 2008; Chauffaille, Bandeira, Silva, 2014). This oncogene encodes the production of a chimeric protein with high tyrosine kinase activity, which is directly related to the pathogenesis of CML (Gora-Tybor, Robak, 2008).

A major breakthrough in the treatment of CML has been achieved with the advent of selective inhibitors of tyrosine kinase such as imatinib mesylate (Glivec) and its derivatives. Despite the good results obtained by these drugs, the lack of response to treatment that occurs when cancer cells develop resistance mechanisms is an important outcome of this disease (Yun *et al.*, 2014; Wang *et al.*, 2015).

Similarly, antimicrobial therapy constitutes a challenge due to the ease with which bacteria acquire resistance genes transmitted by mobile genetic elements (Brown-Jaque, Calero-Cáceres, Muniesa, 2015). Biofilm formation is one of the major virulence factors developed by bacteria. Biofilm is commonly associated with chronic

***Correspondence:** R. Hörner. Laboratório de Bacteriologia, Departamento de Análises Clínicas e Toxicológicas, Centro de Ciências da Saúde, Universidade Federal deSanta Maria (UFSM), Santa Maria,RS. Prédio 26, Sala1201, Campus da UFSM, CEP: 97015-900. Telefax: +55(55) 3220-8751. E-mail: rosmari.ufsm@gmail.com

infections because it resists host defense systems and has increased tolerance to antibiotics and disinfectants (Høiby *et al.*, 2010).

Triazene compounds (TZCs) are characterized by the diazoamine group (N = N-N) (Moore, Robinson, 1986), which accounts for their biological properties (Marchesi *et al.*, 2007). They have a broad pharmacological versatility: antibacterial (Horner *et al.*, 2008; Domingues *et al.*, 2010; Ombaka, Muguna, Gichumbi, 2012; Tizotti *et al.*, 2016), antifungal (Ombaka, Muguna, Gichumbi, 2012), antileukemic (Matheson *et al.*, 2004; Domingues *et al.*, 2010; Bonmassar *et al.*, 2013; Tizotti *et al.*, 2016), and synthetic nuclease (Domingues *et al.*, 2010). Dacarbazina® and Temozolomida® are examples of TZC compounds widely used in the clinical treatment of various malignancies (Bonmassar *et al.*, 2013).

The combination of the pharmacophoric radical TZC with metal ions that have biological activity such as ion gold tends to have a synergistic effect, producing more active and stable molecules (Sreedhara, Cowan, 2001). Thus, this study aimed to synthesize and characterize a new triazenide compound complexed with ion gold (I), as well as to evaluate the *in vitro* antiproliferative and antibacterial activity against the cell line K562 (CML) and bacterial isolates of coagulase-negative staphylococci (CoNS), identified as biofilm producers.

MATERIAL AND METHODS

Synthesis of Au(I) triazenide complex {[(1-(2-bromophenyl)-3-(2-nitrophenyl) triazenide](triphenylphosphine)gold(I)}

Under continuous stirring, the free ligand 1-(2-bromophenyl)-3-(2-nitrophenyl)triazene $C_{12}H_9N_4O_2Br$ (100 mg, 0.311 mmol) was dissolved in a mixture of 20 mL of methanol and tetrahydrofuran (1:1), resulting in a yellow transparent solution. The free ligand was deprotonated by the addition of 5 drops of an alkaline solution of potassium methoxide, previously prepared by dissolution of potassium hydroxide (1000 mg, 17.82 mmol) in 10 mL of methanol. The reaction mixture changed to transparent deep-red. After stirring of the reaction mixture during 30min, triphenylphosphine-gold(I)chloride (154 mg, 0.311 mmol) was added. The color of the reaction mixture changed to orange and an orange-red precipitate was observed. The reaction mixture was filtered-off and the isolated precipitate was dissolved in 10 mL of pyridine. Transparent orange crystals with a block shape and suitable for X-ray diffraction were obtained after 48h by slow evaporation of the solvent, and vacuum-dried in a Schlenk vessel for three days. Yield: {[(1-(2-bromophenyl)-3-(2-nitrophenyl)triazenide] (triphenylphosphine)gold(I)} (0.216 g, 0.227 mmol), 89% based on the employed mass of triphenylphosphine-gold(I) chloride; m.p.: 138 °C; Anal. Calc. for $C_{30}H_{23}AuBrN_4O_2P$: C, 46.23; H, 2.97; N, 7.19%. Found: C, 45.20; H, 2.84; N, 6.83%.

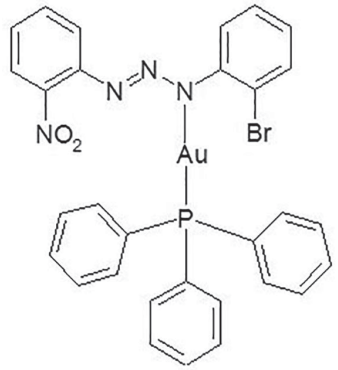

FIGURE 1 - Structure of the triazenide gold (I) complex : {[1- (2-bromophenyl) -3- (2-nitrophenyl) triazenide] (triphenylphosphine) gold (I)}.

Single-crystal X-ray diffraction

A single-crystal sample was attached to a glass wire and was subjected to the collection of diffraction data at room temperature (20-22 °C) with a Bruker APEX II CCD diffractometer, with an area detector and monochromatized Mo-Kα radiation with graphite monochromator (Bruker, 2004). Data integration and absorption correction were performed with SAINT (Bruker, 2004) and SADABS (Sheldrick, 1996) softwares, respectively. Structures were solved by direct methods (Burla *et al.*, 2005) and refined using the square of the structure factor (F2) and complete matrices, with anisotropic thermal parameters for all non-hydrogenic atoms (Sheldrick, 1997). Fractional coordinates of hydrogen atoms of the phenyl rings were obtained geometrically (C-H = 0.93 Å for the C_{SP2} atoms), refined and attached to their respective carbon atoms and isotropic thermal parameters with values U_{iso} (H) relating to $1,2U_{eq}C_{sp2}$. Tables with crystallographic parameters and details regarding data collection were generated with the WinGX program (Farrugia, 1999), and graphical representations of structures and/or structural details discussed were generated with the DIAMOND (Brandenburg, 2005) program.

In vitro antiproliferative activity

Cell culture

The Chronic Myeloid Leukemia K562 cell line,

established from the sample of a 53- year-old patient was commercially acquired at the Cell Bank of Rio de Janeiro - BCRJ, Paul Erlich Technical and Scientific Association - APABCAM. Cells were cultured in Roswell Park Memorial Institute (RPMI) 1640 medium supplemented with 10% fetal bovine serum (Gibco® SBF-), 100 IU/ml penicillin G, 100mg/ml streptomycin for 24 h at 37 °C in a humid atmosphere with 5% carbon dioxide (CO_2).

Cytotoxicity assay

The cytotoxic effect of the complex on the cell line K562 was performed using the colorimetric assay based on the reduction of diazonium salt bromide 3-(4,5-dimethylthiazol-2-yl)-2,5-diphenyltetrazolium bromide (MTT) (Mosmann, 1983). The compound was dissolved in a mixture of ultra-pure water and dimethylsulfoxide DMSO (1:1) and then diluted at different concentrations (100, 50, 25, 12, 6, 3, 1.5 and 0.75 µM). In the cytotoxicity assay, 3 x 10^6 cells/well were used in a 96-well plate exposed to different concentrations of the compound and incubated for 20 h. Control culture containing cells in the absence of the compound was also performed. Imatinib mesylate (Glivec) was the antineoplastic used as reference. After 20h, each well was treated with 20 microliters (uL) of MTT and plates were re-incubated for additional 4h at 37 °C and 5% CO_2. After incubation, formazan crystals were dissolved by addition of DMSO and the inhibition of cell growth detected by measuring absorbance at 570 nanometers (nm) using an Epoch® microplate reader (Fisher BT2000 Bio-Tek). Each test was performed in triplicate in three independent tests. Results were statistically analyzed by SISVAR software (Ferreira, 1988). For cell death values (%), analysis of data variance was performed and means were compared by Tukey test at 5% error probability. IC_{50} values corresponding to the concentration of compound able to inhibit growth of 50% of the cells were analyzed by *GraphPad Prism* 5.

In vitro antibacterial activity

Isolates and bacterial strains

The *in vitro* antibacterial activity of the Au (I) triazenide complex was evaluated against seven CoNS bacterial isolates, obtained from an investigation of contamination in platelet concentrates. These microorganisms have been characterized as biofilm producers by adhesion to a borosilicate tube and Congo red agar phenotypic methods (Christensen *et al.*, 1982; Freeman, Falkiner, Keane, 1989), and by screening for *ica*ACD genes by polymerase chain reaction (PCR) (Arciola *et al.*, 2005). Isolates were two *Staphylococcus epidermidis*, one *Staphylococcus saprophyticus,* three *Staphylococcus haemolyticus* and one *Staphylococcus warneri*. Two strains of international reference standard (American Type Culture Collection - ATCC) of non-biofilm-producing *Staphylococcus epidermidis* 12228 and *Staphylococcus saprophyticus* 15305 were also used.

Determination of the minimum inhibitory concentration (MIC)

Bacterial isolates and ATCC strains, stored in 15% glycerol at -80 °C, were pre-activated using the agar trypticase soy medium (TSA) for 24 h at 35 ± 2 °C. Evaluation of antibacterial activity of the compound was performed using the conventional method of broth microdilution for Minimum Inhibitory Concentration (MIC) based on the Clinical and Laboratory Standards Institute guidelines (CLSI, 2012). The test compound was diluted in DMSO and ultra-pure water (1:1) at a concentration of 2560 µg mL^{-1} and then successive dilutions were made with concentrations from 128 to 0.25 µg mL^{-1}. The bacterial inoculum was prepared using a 0.5 McFarland scale, so that each well contained 5 x 10^5 CFU mL^{-1}. Plates were incubated for 24 h at 35 ± 2 °C and after this period, the MIC was determined visually as the lowest concentration that completely inhibited growth of microorganisms in dilution wells. Each assay was performed in triplicate.

ETHICAL CONSIDERATIONS

This study was approved by the Research Ethics Committee (CEP) of UFSM, under the certificate number of presentation for ethical consideration (CAAE) 0285.0.243.000-09.

RESULTS AND DISCUSSION

Crystal structure

Glassy crystals with orange prismatic habit were obtained from slow evaporation of the stock solution. Values of the unit cell parameters were obtained based on the refinement of reflections obtained in different quadrants of Ewald sphere, related to the angular region and refined by the least squares method at the end of the collection of intensity data. Crystallographic parameters and further details regarding the collection of data and refinement of the complex are listed in Table I.

The geometry of the Au (I) triazenide complex is linear, with a ligand triazenide [Au-N13 = 2.075 (3) Å]

TABLE I - Data from intensity collection and refinement of the crystal/molecular structure of the Au (I) triazenide complex

Crystallography Parameters	Au (I) triazenide complex
Molecular Formula	$[Au(C_{12}H_8N_4O_2Br)(C_{18}H_{15}P)]$
Molecular Mass (g)	779,37
Color/Shape	Orange / Prism
Dimensions (mm)	0,18X 0,15 X 0,08
Lattice System	Monoclinic
Space Group	$P2_1/n$ (n°. 14)[a]
Unit cell parameters	a = 8,7887(10) Å b = 11,2594(2) Å c = 28,3257(4) Å α = 90° β = 92,9570(10) ° γ = 90°
Volum	2799,25(7) Å^3
Z	4
Density (calculated)	1,849 mg/m^3
F(000)	1504
Wavelenght/Radiation	0,71073 Å / Mo-K_α
Absorption coeficiente	6,775 mm-1
Θ Range	2,39 a 28,29 °
Index Range	-11 ≤ h ≤ 11 -15 ≤ k≤ 12 -36 ≤ l ≤ 37
Structure Solution	Direct Methods (SIR-2004)
Structure refinement	SHELXL-97
Refining methods	Least squares,complete matrix including F^2
Reflections collected	26152
Reflections observed	6939 [$R_{(int)}$ =0,0460]
Reflexões observadas	4912
Data/restraints/Parameters	6939 / 0 / 352
Goodness-of-fit on F^2	1,040
Final $R_{indices}$ [I>2σ(I)]	R_1 =0,0333 wR_2 = 0,0656
R indices (all data)	R_1 = 0,0587 wR_2 = 0,0729
Largest Diff (Peak and Hole)	1,116[b] e -1,198[c] e.Å^3

[e](1,12 e.Å^3) for 0,9867; 0,0787; 0,2291 [1.01 Å of Br]. [f](-1,20 e.Å^3) for 0,7871; 0,1271; 0,2339 [0.84 Å of Br]

and a neutral molecule triphenylphosphine [Au-P = 2.224 (11) A] bound to the gold ion with an angle [N13-P-Au = 178.72 (9) °] near 180 °, confirming the linearity, as shown in Figure 2.

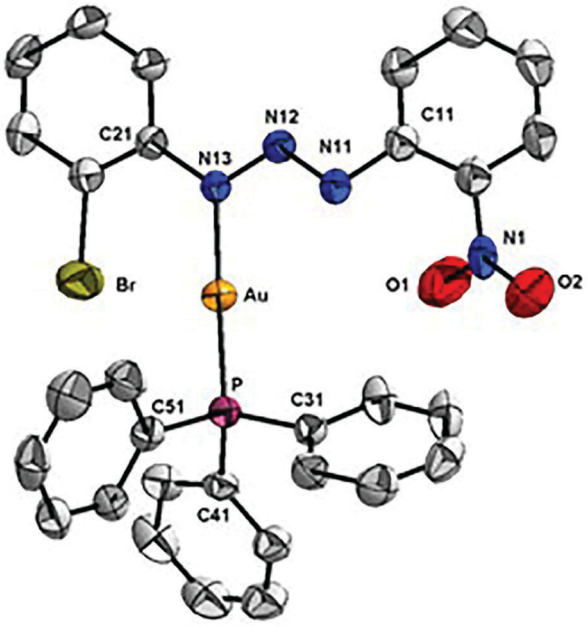

FIGURE 2 - Triazenide gold complex structural projection (I). Thermal ellipsoids with probability level of 50%. Hydrogen atoms omitted for better viewing.

In the solid state, the structure of the complex is formed by non-classic aromatic hydrogen bonds type C-H ··· M (where M represents the centroid point of the aromatic ring). These interactions involve a polarized hydrogen atom of a C-H group donor of a phenyl ring of triphenylphosphyne in a unit of a molecular complex, and an acceptor ring of another phenyl of triphenylphosphyne, resulting in the formation of centrosymmetric dimers. These dimers are reproduced by the same type of interaction, forming a supramolecular arrangement 1- D.

This complex fragments involved in the determination of these interactions are C31-C36 / C56'-C51' for the formation of centrosymmetric dimers, as represented in Figure 3.

In addition to the previous determinations, it is necessary to determine the angles and distances between the two rings. These distances and angles are listed in Table II. The centrosymmetric dimers of the complex, formed by aromatic interactions, are projected in Figure 4.

These centrosymmetric dimers in the structure of the complex are reproduced by aromatic interactions (C-H ··· Ph), resulting in supramolecular 1-D arrangements via non-classical aromatic centrosymmetric hydrogen bonds C-H ··· M (M = centroid of the ring) between the triphenylphosphine phenyls, both in the crystallographic direction [100].

The fragments considered in these interactions are C41-C46 / C51 '- C56' '[symmetry Codes (' '):

TABLE II - Geometric parameters for the non-classical aromatic hydrogen bonds (C-H ··· Ph) of the complex dimers

D–H···A	D···A (Å)	H···A (Å)	<D–H···A (°)	D(M) (Å)	d(M) (Å)	<Ph–H–M (°)
C32–H32···C56'	C32···C56'	H32···C56'	C32–H32···C56'	C32···M	H32···M	C32–H32···M
	3,836	3,076	140,06	3,946	3,363	122,61

M = centroid point of the aromatic ring. [Symmetry codes: ('): x-1, y-2, z)].

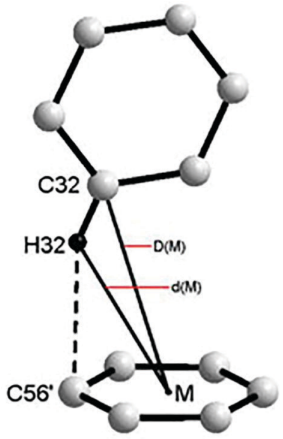

FIGURE 3 - Projection of fragments involved in the non classical aromatic hidrogen bondings C-H ··· Ph of the dimers of the C31-C36 / C51'-C56 'complex. [Symmetry Code x-1, y-2, z]. Hydrogen atoms are omitted for better layout view. M = centroid point of the aromatic ring.

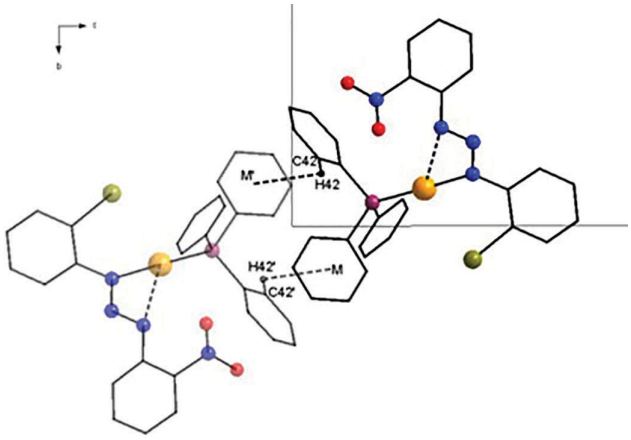

FIGURE 4 - Projection of the centrosymmetric dimers of the complex, in the crystallographic direction of the α axis, formed by non-classical aromatic hydrogen bonds C-H ··· M (where M is the centroid point of the aromatic ring C51'-C56 '). Hydrogen atoms are omitted for better viewing. Showing partial cell content. [Symmetry Code ('): x-1, y-2, z]. [Código de simetria ('): 1-x, 2-y, -z].

-1 + x, y, z]. Figure 5 shows the considered fragments with all denominations, which are essential to determine interactions, and these values are described in Table III.

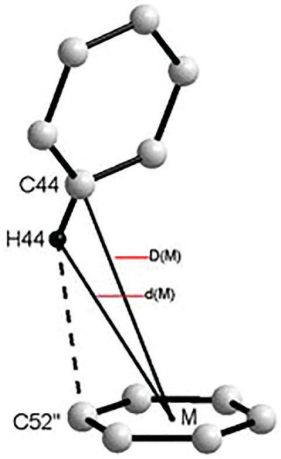

FIGURE 5 - Projection of fragments involved in non-classical aromatic hydrogen bonding C-H ··· Ph on C41-C46 / C51' - C56' complex. [Symmetry Codes ('): -1 + x, y, z]. Hydrogen atoms are omitted for better layout view. M = centroid point of the aromatic ring.

Figure 6 depicts the projection of the supramolecular arrangement of the complex formed by centrosymmetric dimers reproduced in a 1-D chain via non-classical aromatic centrosymmetric hydrogen bonds (C-H ··· Ph) in the crystallographic direction [100].

Biological activity

When produced by microorganisms, biofilm protects against host defense mechanisms, preventing or hindering the diffusion of antimicrobials (Høiby *et al.*, 2010). The concentration of antibiotic required to combat infections caused by biofilm- producing microorganisms can be up to a thousand times higher compared to infections caused by their planktonic counterparts (non-biofilm producers) (Musk, Hergenrother, 2006; Høiby *et al.*, 2010).

The tested compound showed significant antibacterial activity when compared to non-biofilm-producing strains. The results of this activity are shown in Table IV. It can be observed that among the seven biofilm-producing clinical isolates, all had MICs lower or equal to those of strains that do not produce biofilm. A study by Presterl and colleagues (2009) has shown that bacterial isolates of biofilm-

TABLE III - Geometric parameters for the non-classical aromatic hydrogen bonds (C-H ··· Ph) of the 1-D arrangement of the complex

D–H···A	D···A (Å)	H···A (Å)	<D–H···A (°)	D(M) (Å)	d(M) (Å)	<Ph–H–M (°)
C44–H44···C52”	C44···C52”	H44···C52”	C44–H44···C52”	C44···M	H44···M	C44–H44···M
	3,658	2,821	150,43	3,911	3,291	126,03

M = centroid point of the aromatic ring. [Symmetry codes: (‘’): -1 + x, y, z].

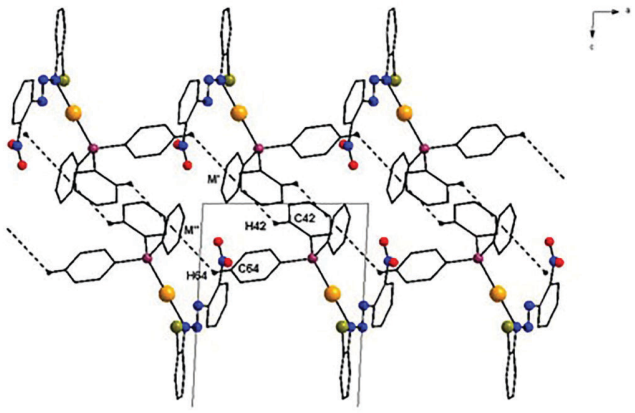

FIGURE 6 - Projection of the supramolecular arrangement of the complex in the crystallographic direction of the axis b, formed by non-classical aromatic hydrogen bondings C54-H54 ··· M " (where M is the centroid point of the aromatic ring C51 " - C56 '). Hydrogen atoms are omitted for better visualization. Showing partial cell content. [Symmetry code ('): -1 + x, y, z].

TABLE IV - Antibacterial activity profile of (1-(2-bromophenyl)-3-(2-nitrophenyl) triazenide] (triphenylphosphine) gold (I) against biofilm producing CoNS isolates

Microorganisms	MIC (µg/mL)
Staphylococcus epidermidis	=32
Staphylococcus epidermidis	=32
Staphylococcus saprophyticus	=32
Staphylococcus haemolyticus	=64
Staphylococcus haemolyticus	=32
Staphylococcus haemolyticus	=64
Staphylococcus warneri	=64
Staphylococcus epidermidis ATCC 12228*	=64
Staphylococcus saprophyticus ATCC 15305*	=64

*Non-biofilm producing ATCC strains.

producing *S. epidermidis* have increased resistance to antibiotics. These researchers evaluated the combination of azithromycin at a concentration of 512 µg/ml with high concentrations of ceftriaxone, showing a significant bactericidal effect (Presterl *et al.*, 2009). The studied Au (I) triazenide complex proved to be more active, compared to these antimicrobial agents, being capable of inhibiting all isolates of biofilm-producing *S. epidermidis*, at a concentration four times lower (32 µg/mL).

Several studies using TZC compounds have shown that these compounds have broad antimicrobial activity (Hörner *et al.* 2008; Domingues *et al.*, 2010; Ombaka *et al.*, 2012; Paraginski *et al.*, 2014; Tizotti *et al.*, 2016). Studies suggest that the antibacterial action of TZCs is due to the chelating activity of metal ions that are constituents of the bacteria cell wall, hindering their synthesis and leading to cell death (Hörner *et al.* 2008; Ombaka *et al.*, 2012). According to Paraginski and colleagues, complexation of TZC compounds with metal ions such as gold (I) can provide potent antibacterial activity (Paraginski *et al.*, 2014). However, this is, to the best of our knowledge, the first study to use such compounds complexed with metals like gold against biofilm-producing microorganisms isolated from platelet concentrates.

In a study using gold nanoparticles against multidrug-resistant bacteria, it has been observed that they act altering membrane potential and decreasing the synthesis of adenosine triphosphate (ATP), causing a general decline in bacterial metabolism (Cui *et al.*, 2012). Barreiro *et al.* (2012) reported that this metal acts inhibiting bacterial proliferation by blocking cell cytokinesis (Barreiro *et al.*, 2012).

Domingues *et al.* (2010), obtained MIC values>128 mg/mL using TZCs not complexed with metal compounds against an *S. epidermidis* clinical isolate, as well as *S. epidermidis* ATCC 12128 strain (Domingues *et al.*, 2010). In addition, another study using 15 TZC compounds not associated with metal showed MIC values=64 mg/mL for hospital isolates of *S. epidermidis* and *S. saprophyticus* (Horner *et al.*, 2008). In both studies, the compounds showed lower activity compared to Au (I) triazenide. Thus, we believe that part of the significant antibacterial activity demonstrated is due to the complexation of TZC with metal, which potentiates its action.

As for the anti-proliferative activity, we can see the percentage of cell death obtained by the compound, as shown in Table V. We observed that the compound

TABLE V – Antiproliferative activity of compound {(1-(2-bromophenyl)-3-(2-nitrophenyl) triazenide] (triphenylphosphine) gold (I)} against K562 cells

Concentration (µM)	TZC Complex Au (I) triazenide complex		Imatinib mesylate	
	% Cell death	IC_{50} (µM)	% Cell death	IC_{50} (µM)
100	49.77ab	4.96	60,35b	3,86
50	60.18c		56,60b	
25	58.16c		57,05b	
12	57.71c		54,81b	
6	52.12b		54,36b	
3	50.00ab		57,61b	
1.5	48.99ab		55,82b	
0.75	47.54[a]		41,83[a]	
Media	53.06		54,8	
CV (%)	2.66		4,4	

Means followed by the same letter do not differ by Tukey test at 5% error probability ($p<0.05$). Coefficient of variation (CV).

activity was not dose-dependent, being more active in the concentration of 50 uM, which was also evidenced by Domingues *et al.* (2010) in trials with TZCs against AML cells (Domingues *et al.*, 2010). In addition, concentrations of 50, 25 and 12 µM showed no significant difference through the statistical analysis of results, as well as the concentrations of 100, 3 and 1.5 µM. Imatinib Mesylate (Glivec) showed no significant difference in the established concentrations, except for the concentration of 0.75 µM. Regarding IC50, we found that the Au (I) triazenide complex showed cytotoxicity value lower than imatinib mesylate (Glivec), which is the standard drug used for the treatment of CML.

According to Marchesi *et al.* (2007), the cytotoxic action of TZCs occurs by methylation of the O_6 position of a guanine base of DNA, mediated by methyldiazonium ion (N + CH3 N), a highly reactive derivative of these compounds. For this reason, guanine loses the ability to bind to cytosine, creating an incorrect pair of bases, for the methylated guanine preferentially binds to thymine (Marchesi *et al.*, 2007).

Primary studies have shown that TZC compounds may have their activity related to the inhibition of the tyrosine kinase enzyme (Matheson *et al.*, 2004), which is directly related to the malignancy of CML (Gora-Tybor, Robak, 2008). Furthermore, it is known that the acquired resistance to tyrosine kinase inhibitors have been a problem for several patients with this malignancy (Yun *et al.*, 2014; Wang *et al.*, 2015).

In clinical practice, drugs bound to this metal have been especially studied in cultured cells systems, where it is possible to assess their cytotoxic potential (Gouvea *et al.*, 2012; Bertrand, Casini, 2014). Gold organometallic compounds play an important role in medicinal chemistry, and these studies were determinant to trigger an enormous interest in the scientific community for new complexes of this metal, aiming their application to antitumor therapy (Bertrand, Casini, 2014), rheumatoid arthritis therapy, and viral and parasitic diseases (Berners-Price, Filipovska, 2011).

CONCLUSION

A new gold(I) triazenide complex, namely {[(1-(2-bromophenyl)-3-(2-nitrophenyl)triazenide] (triphenylphosphine)gold(I)} was synthetized and fully characterized including the X-ray single crystal structure analysis demonstrating its undoubted molecular structure in the solid state.

According to the results, we suggest that the significant biological activity demonstrated by the Au (I) triazenide complex studied is due to the presence of gold ion which enhances the action of diazoamine group. Moreover, this research is part of an initial study, the first investigation to use Au (I) triazenide complex against K562 cells and biofilm-producing bacteria. As a result, other analyses are being carried out through the synthesis of new TZC compounds complexed with metals, as well as the elucidation of the possible mechanisms of action.

ACKNOWLEDGMENTS

This work received financial support from CNPq (Proc. 485262/2013-4). We would like to thank CNPq (Proc. 305254/2009-0) (M.H.) for the grant.

SUPPLEMENTARY MATERIAL

CCDC 1483264 contains the supplementary crystallographic data for this paper. These data can be obtained free of charge from The Cambridge Crystallographic Data Centre via www.ccdc.cam.ac.uk/data_request/cif.

REFERENCES

Arciola CR, Gamberini S, Campoccia D, Visai L, Speziale P, Baldassarri L, et al. A multiplex PCR method for the detection of all five individual genes of ica *locus* in *Staphylococcus epidermidis*. A survey on 400 clinical isolates from prosthesis-associated infections. J Biomed Mater Res. 2005;75(2): 408-413.

Barreiro E, Casas JS, Couce MD, Sánchez A, Seoane R, Estévez AP, et al. Synthesis and antimicrobial activities of gold(I) sulfanylcarboxylates. Gold Bull. 2012;45(1):23-34.

Berners-Price SJ, Filipovska A. Gold compounds as therapeutic agents for human diseases. Metallomics. 2011;3(9):863-873.

Bertrand B, Casini A. A golden future in medicinal inorganic chemistry: the promise of anticancer gold organometallic compounds. Dalton Trans. 2014;43(11):4209-4219.

Bonmassar L, Marchesi F, Pascale E, Franzese O, Margison GP, Bianchi A, et al. Triazene compounds in the treatment of acute myeloid leukemia: a short review and a case report. Curr Med Chem. 2013;20(9):2389-2401.

Brandenburg K. DIAMOND. 2004-2005, Version 3.1. Bonn, Germany: Crystal impact GbR; 2005.

Brown-Jaque M, Calero-Cáceres W, Muniesa M. Transfer of antibiotic resistance genes via
phage-related mobile elements. Plasmid. 2015;79:1-7.

Bruker. APEX2 (Version 1.0.22), COSMO (Version 1.48), SAINT (Version 7.06A). Madison, Wisconsin, USA: Bruker AXS Inc.; 2004.

Burla MC, Caliandro R, Camalli M, Carrozzini B, Cascarano GL, De Caro L, et al. SIR2004 – an improved tool for crystal structure determination and refinement. J Appl Cryst. 2005;38:381-388.

Chauffaille MLLF, Bandeira ACA, Silva ASG. Diversity of breakpoints of variant Philadelphia chromosomes in chronic myeloid leukemia in Brazilian patients. Rev Bras Hematol Hemoter. 2014;37(1):17-20.

Christensen GD, Simpson WA, Bisno AL, Beachey EH. Adherence of slime producing strains of *Staphylococcus epidermidis* to smooth surfaces. Infect Immun. 1982;37(1):318-326.

Clinical Laboratory Standards Institute. CLSI. Methods for dilution antimicrobial susceptibility tests for bacteria that grow aerobically; Approved Standart. CLSI document M07-A9. 9th ed. Wayne, PA: CLSI; 2012.

Cui Y, Zhao W, Tian Y, Zhang W, Lü X, Jiang X. The molecular mechanism of action of bactericidal gold nanoparticles on *Escherichia coli*. Biomaterials. 2012;33(7):2327-2333.

Domingues VO, Hörner R, Reetz LGB, Kuhn F, Coser VM, Rodrigues JN, et al. In vitro evaluation of triazenes: DNA cleavage, antibacterial activity and cytotoxicity against acute myeloid leukemia cells. J Braz Chem Soc. 2010;21(12):2226-2237

Farrugia LJ. WinGX - an integrated system of windows programs for solution, refinement and analysis of single crystal x-ray diffraction data, vers. 1.64.04. J Appl Cryst. 1999;32:837-838.

Ferreira DF. SISVAR - sistema de análise de variância para dados balanceados. Lavras: UFLA; 1988. 19 p.

Freeman DJ, Falkiner FR, Keane CT. New method for detecting slime production by coagulase negative *Staphylococci*. J Clin Pathol. 1989;42(8):872-874.

Gora-Tybor J, Robak T. Targeted drugs in chronic myeloid leukemia. Curr Med Chem. 2008;15(29):3036-3051.

Gouvea LR, Garcia LS, Lachter DR, Nunes PR, Pereira FC, Silveira-Lacerda EP, et al. Atypical fluoroquinolone gold(III) chelates as potential anticancer agents: relevance of DNA and protein interactions for their mechanism of action. Eur J Med Chem. 2012;55:67-73.

Heim S, Mitelman F. Cancer cytogenetics. 3 ed. New Jersey: Wiley-Blackwell; 2009. 736 p.

Høiby N, Bjarnsholt T, Givskov M, Molin S, Ciofu O. Antibiotic resistance of bacterial biofilms. Int J Antimicrob Ag. 2010;35(4):322-332.

Hörner M, Giglio VF, Santos AJRWA, Westphalen AB, Iglesias BA, Martins PR, et al. Triazenes and antibacterial activity. Rev Bras Ciênc Farm. 2008;44(3):441-449.

Marchesi F, Turriziani M, Tortorelli G, Avvisati G, Torino F, Vecchis L. Triazene compounds: mechanism of action and related DNA repair systems. Pharmacol Res. 2007;56(4):275-287.

Matheson SL, McNamee JP, Wang T, Alaoui-Jamali MA, Tari AM, Jean-Claude BJ. The combi-targeting concept: dissection of the binary mechanism of action of the combi-triazene SMA41 in vitro and antitumor activity in vivo. J Pharmacol Exp Ther. 2004;311(3):1163-1170.

Moore DS, Robinson SD. Catenated nitrogen ligands part I. Transition metal derivatives of triazenes, tetrazenes, tetrazadienes, and pentazadienes. Adv Inorg Chem Radiochem. 1986;30:1-68.

Mosmann T. Rapid colorimetric assay for cellular growth and survival: application to proliferation and cytotoxicity assay. J Immunol Methods. 1983;65(1-2):55-63.

Musk DJJr, Hergenrother PJ. Chemical countermeasures for the control of bacterial biofilms: effective compounds and promising targets. Curr Med Chem. 2006;13(18):2163-2177.

Ombaka AO, Muguna A T, Gichumbi JM. Antibacterial and antifungal activities of novel hydroxytriazenes. J Environ Chem Ecotoxicol. 2012;4(7):133-136.

Paraginski GL, Berticelli CR, Zambiazi PJ, Paraginski VTK, Hörner M, Santos AJRWA, et al. In vitro antibacterial activity and toxicity toward *Artemia salina Leach*. of some triazene compounds. Quím Nova. 2014;37(7):1138-1444.

Presterl E, Hajdu S, Lassnigg AM, Hirschl AM, Holinka J, Graninger W. Effects of azithromycin in combination with vancomycin, daptomycin, fosfomycin, tigecycline, and ceftriaxone on staphylococcus epidermidis biofilms. Antimicrob Agents Chemother. 2009;53(8):3205-3210.

Sheldrick GM. SADABS - Program for empirical absorption correction of area detector data. Germany: University of Göttingen; 1996.

Sheldrick GM. SHELXL-97 - Program for crystal structure refinement. Germany: University of Göttingen; 1997.

Sreedhara A, Cowan JA. Catalytic hydrolysis of DNA by metal ions and complexes. J Biol Inorg Chem. 2001;6(4):337-347.

Tizotti MK, Hörner R, Freitas AGO, Kempfer CB, Bottega A, Rodrigues JN, et al. X-ray characterization and in vitro biological evaluation of 1-(4-amidophenyl)-3-(4-acetylphenyl)triazene and the gold(I) triazenide complex {Au(I)[RPhNNNPhR′][PPh3]} [R = (C O)NH2, R′ = (C O)CH3]. Inorg Chim Acta. 2016;441:78-85.

Wang W, Jianfeng Z, Li Y, Yang X, Ele Y, Tingting L, et al. Divalproex sodium enhances the anti-leukemic effects of imatinib in chronic myeloid leukemia cells partly through SIRT1. Cancer Lett. 2015;356(2 pt B):791-799.

Yun SM, Jung KE, Kim SJ, Fang Z, Son MK, Yan HH, et al. HS-438, a new inhibitor of imatinib-resistant BCR-ABL T315I mutation in chronic myeloid leucemia. Cancer Lett. 2014;348(1-2):50-60.

Received for publication on 10th November 2016
Accepted for publication on 15th April 2017